NJC
New Journal of Chemistry
A journal for new directions in chemistry

Accepted Manuscript

This article can be cited before page numbers have been issued, to do this please use: C. S. Abeywickrama, K. M. Arachchige, K. J. Wijesinghe, R. V. Stahelin and Y. Pang, *New J. Chem.*, 2025, DOI: 10.1039/D4NJ05398B.

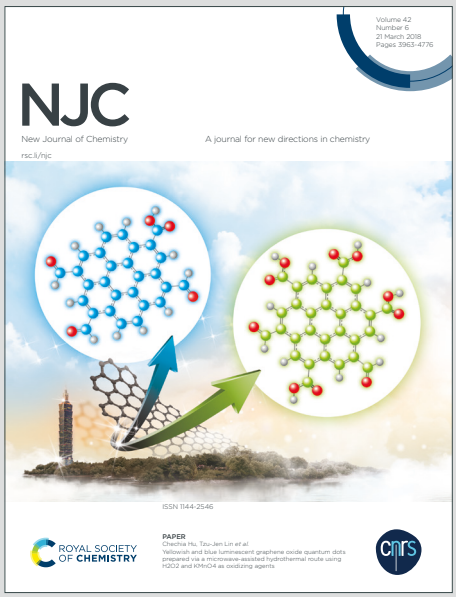

ROYAL SOCIETY OF CHEMISTRY

rsc.li/njc

View Article Online
DOI: 10.1039/D4NJ05398B

COMMUNICATION

A Large Stokes' Shift Styryl Pyridinium Derivative with a Stable Green-emission for Mitochondria Imaging in Live Cells

Received 00th January 20xx,
Accepted 00th January 20xx

DOI: 10.1039/x0xx00000x

Chathura S. Abeywickrama,*[a] Kavinda M. Arachchige,[a] Kaveesha J. Wijesinghe, [b] Robert V. Stahelin, [c] and Yi Pang [d]

Green-emitting styryl pyridinium probe (EPN) was developed for live-cell imaging applications. EPN exhibited a large Stokes shift (Δλ ≈150 nm) due to efficient ICT across π-acceptor system. Probe exhibited exceptional biocompatibility and excellent specificity to cellular mitochondria. EPN exhibited a great photostability to continuous irradiation and exhibited a stable emission in cells up 5 hours post-staining.

Small-molecule fluorescent imaging dyes are versatile tools for visualizing complex biological environments.[1–4] Recent advancements in fluorescence microscopy techniques that reach high spatial resolution (i.e., super-resolution) have unlocked the potential of biomedical imaging at the molecular level.[5–7] Long-lasting, bright, and highly biocompatible imaging dyes are ideal for visualizing living systems. Probes with well-resolved excitation-emission profiles (i.e., large Stokes' shift) can effectively mitigate issues such as self-quenching of fluorophore and bleed-through interferences that occurs during imaging.[4,8] Recently, several interesting large Stokes' shift (Δλ ≈100-200 nm) imaging dyes have been developed within the red to near-infrared emission region.[9–12] Excited-state intra-molecular proton transfer (ESIPT) and intramolecular charge transfer (ICT) are two key photophysical phenomena that have been utilized to develop such large Stokes' shift imaging dyes.[4,13,14] Undoubtedly, the development of red and NIR emitting probes has distinct advantages in biomedical imaging research due to their higher penetration ability through biological tissues. However, many imaging experiments demand multi-color fluorescent labels to distinguish multiple components in complex biological environments. Therefore, the development imaging probes with favourable properties for imaging in the blue-green region is still critical for visualization purposes. Many existing blue-green emitting imaging dyes exhibit inherent narrow Stokes' shifts (Δλ <20 nm), high cytotoxicity, and weak photostability which limits their application in long-term imaging sessions. In this work, we are reporting an interesting green-emitting π-acceptor (π-A) type imaging probe (EPN) with a large Stokes' shift (Δλ ≈100-150 nm) for mitochondria imaging in live cells. **EPN** exhibited an excellent photostability and biocompatibility as a promising imaging candidate.

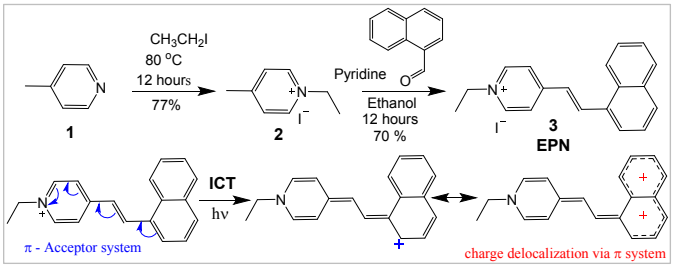

Scheme 1. Synthesis and intramolecular charge transfer (ICT) in **EPN**.

Synthesis. EPN (3) was synthesized in good yields by the condensation of 1-napthaldehyde with pyridinium salt **2** as shown in the Scheme 1. **EPN** was characterized by NMR spectroscopy and high-resolution mass spectrometry (ESI Figures **S1**).

Table 1. Photophysical properties of EPN

Solvent	Toluene	DCM	$CHCl_3$	DMSO	EtOH	Water
λ_{abs} (nm)	390	395	394	388	391	373
λ_{em} (nm)	490	518	507	533	514	525
Δλ (nm)	100	123	113	145	123	152
Φ_{fl}	0.002	0.025	0.018	0.036	0.044	0.011
ε($M^{-1}cm^{-1}$)	8172	10458	10940	9888	10170	9426

[a] Department of Pharmaceutical Sciences, University of Connecticut, Storrs, CT 06269, USA.
[b] Department of Chemistry, University of Colombo, Colombo 00300, Sri Lanka.
[c] Borch Department of Medicinal Chemistry and Molecular Pharmacology, Purdue University, West Lafayette, IN 47907, USA.
[d] Department of Chemistry, University of Akron, OH 44325, USA.
† Footnotes relating to the title and/or authors should appear here.
Supplementary Information available: [details of any supplementary information

View Article Online
DOI: 10.1039/D4NJ05398B

Optical Properties. Photophysical properties of **EPN** was studied in different solvents and summarized in the Table 1 and Figure 1. The absorbance spectra were observed at λ_{abs} ≈370 – 395 nm (Table 1). The absorbance spectra of **EPN** exhibited a moderate- blue shift in polar solvents (i.e., λ_{abs} ≈370 in water) in comparison to non-polar solvents (i.e., λ_{abs} ≈395 in DCM) indicating a hypsochromic character (Figure 1a). However, the emission of **EPN** did not exhibit such noticeable trend (Figure 1b). The emission of **EPN** found to be in the range λ_{em} ≈490- 533 nm (i.e., blue-green region) with calculated fluorescent quantum yields (ϕ_{fl}) 0.002 – 0.044 (Table 1). In comparison to other solvents, the emission of **EPN** in Toluene found to be significantly weaker (ϕ_{fl} ≈0.002) thus can be explained by considering the characteristic "collisional quenching" properties of the solvent due to strong vibrational relaxations. The calculated Stokes' shift was recorded from Δλ ≈100 -150 nm while moving from non-polar to polar environments indicating stronger ICT effect in polar solvent environments that increases the Stokes' shift.

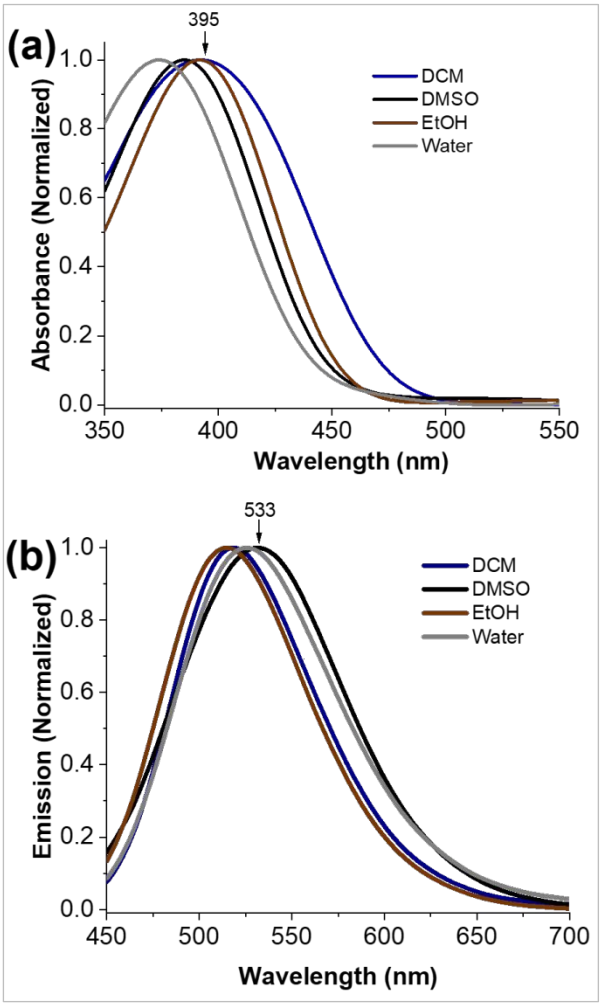

Figure 1. Absorbance (a) and emission (b) of **EPN** (1 x 10^{-5} M) in different solvent environments a 25 °C. **EPN** was excited at 390 nm and the emissions were collected from 420 nm – 700 nm.

Low-temperature Studies. The large Stokes' shift of **EPN** (Δλ ≈100 -150 nm) can be attributed to the extended conjugation across naphthalene which further stabilize strong intramolecular charge transfer (ICT) from naphthalene (π system) to a styryl pyridinium acceptor group as shown in the scheme 1. To evaluate the impact of the ICT, an ethanolic solution of **EPN** was frozen in liquid nitrogen to limit the molecular motion and bond rearrangements associated with the ICT process. While **EPN** was frozen under the ethanol matrix at ultra-low temperature (i.e., -188 °C), probe exhibited the emission at λ_{em} ≈456 nm (Figure 2). When the temperature was increased to room temperature (i.e., 25 °C), the emission peak was red-shifted λ_{em} ≈456 nm (Figure 2). The observed large spectral shift (Δλ ≈58 nm, from 456 nm to 514 nm), in response to the temperature change indicated the impact of strong ICT interaction (Scheme 1).

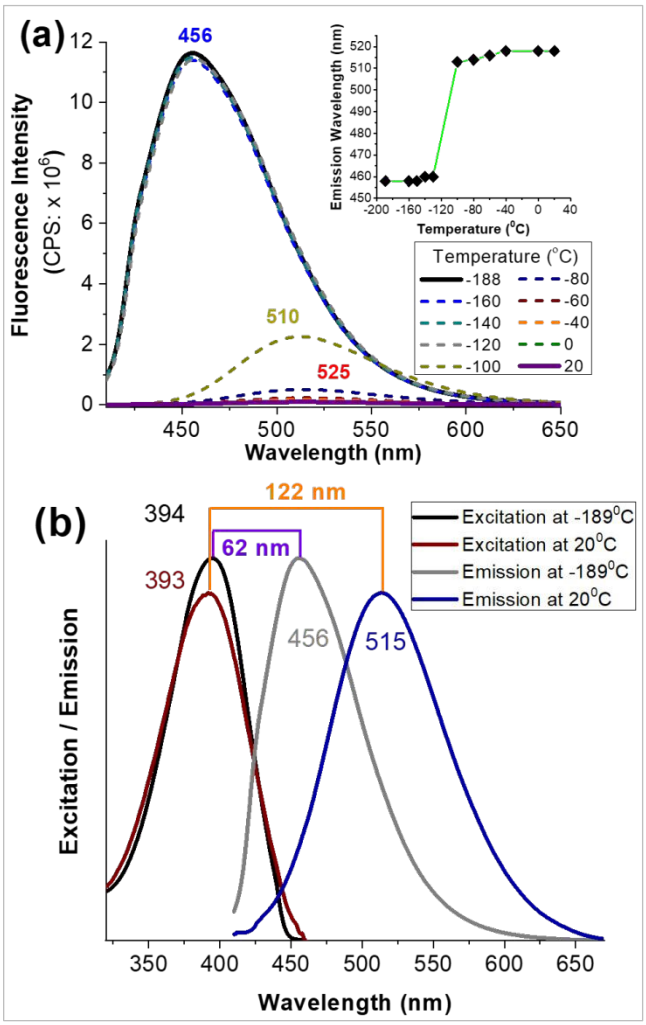

Figure 2. (a)-Fluorescence spectra of **EPN** (1 × 10^{-6} M) in EtOH at low temperature. Inset at the top shows the emission of **EPN** as a function of temperature. **EPN** was excited at 390 nm to acquire the emission. (b)- represents the Normalized excitation and fluorescence spectra at low temperature for **EPN** (1 × 10^{-6} M) in EtOH.

Live cell imaging. The observed interesting photophysical properties encouraged us to investigate the potential of **EPN** as a live cell imaging probe. Thus, HepG2 cells (human hepatocellular carcinoma cell line) and A-172 cells (Human glioblastoma cell line) were stained

with **EPN** (2-4 µM) and visualized by fluorescence confocal microscopy (Figure 3 and ESI Figures S6-S7). Interestingly, cells stained with **EPN** exhibited a strong emission signal while exhibiting a non-uniform tubular network-like staining pattern indicating internalization into a specific cellular compartment. The resulted fluorescence confocal microscopy images did not exhibit a noticeable background signal which suggested probe's suitability as a potential imaging dye. Based on our familiarity with the observed imaging pattern, we hypothesized that **EPN** internalized into cellular mitochondria. The positively charged nature of the **EPN** further supported our hypothesis as many positively charged fluorescent dyes have exhibited potential to localized into cellular mitochondria.

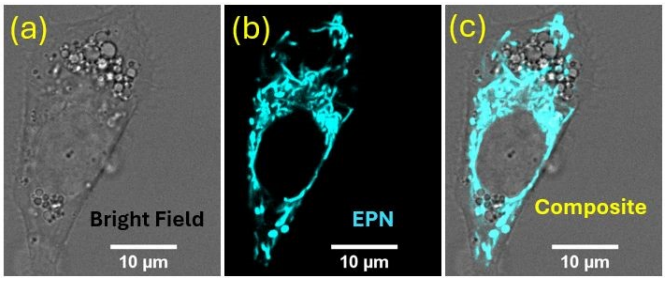

Figure 3. Fluorescence confocal microscopy images of HepG2 cells stained with **EPN** (4 µM) for 30 minutes. Stained cells were excited with 405 nm laser line and the emission was collected from 480 nm to 560 nm.

To confirm sub-cellular specificity of **EPN**, fluorescence confocal microscopy colocalization imaging experiments were performed in HepG2 cells in the presence of a commercial mitochondria marker (i.e., MitoTracker™ Red FM: λ_{ex} ≈579 nm, λ_{em} ≈579 nm). **EPN** exhibited an excellent colocalization (calc. Pearson's colocalization constant =0.9) with MitoTracker™ Red indicating probe's mitochondria specificity (Figure 4). Observed excellent mitochondria specificity of **EPN** provides compelling evidence to support its application as a versatile Mitochondria imaging probe. Considering well resolved excitation and emission spectra profiles (λ_{ex} ≈400 nm, λ_{em} ≈520 nm) that produce a large Stokes' shift (Δλ ≈100 -150 nm) due to strong ICT effect, **EPN** can be efficiently co-stained with any blue green to red emissive fluorescent marker (λ_{ex} ≈ range from 450 nm to 700 nm) without producing any signal interference (i.e., channel bleeding). **EPN** was also exhibit exceptional stability in live cell imaging where probe was evaluated for imaging mitochondria in HepG2 cells up to 5 hours (Figure 5). Probe exhibited a stable emission from stained cells without any noticeable reduction in emission signal (Figure 5a). To further evaluate the photostability of the probe, HepG2 cells stained with **EPN** (4 µM) was continuously irradiated with 405 nm laser line (0.4 mW power) at 2-minute intervals up to 30 minutes. Based on the collected fluorescence microscopy images, the percentage fluorescence recovered (average) was plotted as a function of the irradiation time (Figure 5b). the calculated percentage recovery of the fluorescence found to be over ~85 % of for **EPN** after 16 irradiation cycles which provides convincing evidence to its high photostability as a blue-green imaging dye. To further validate the suitability of **EPN** for live-cell imaging experiments, biocompatibility of the probe was evaluated by cell viability measurements (Figure 5c). Interestingly, **EPN** did not exhibit any noticeable cytotoxicity up to 10 µM concentration based on the viability assessment confirming probe's suitability as a biocompatible mitochondria marker. Also, the laser irradiation (405 nm) experiments performed in **EPN**-stained A-172 cells did not show any noticeable morphological changes in bright-field or dark-field confocal microscopy images suggesting no potential phototoxicity effect at current staining concentrations (ESI Figure S8).

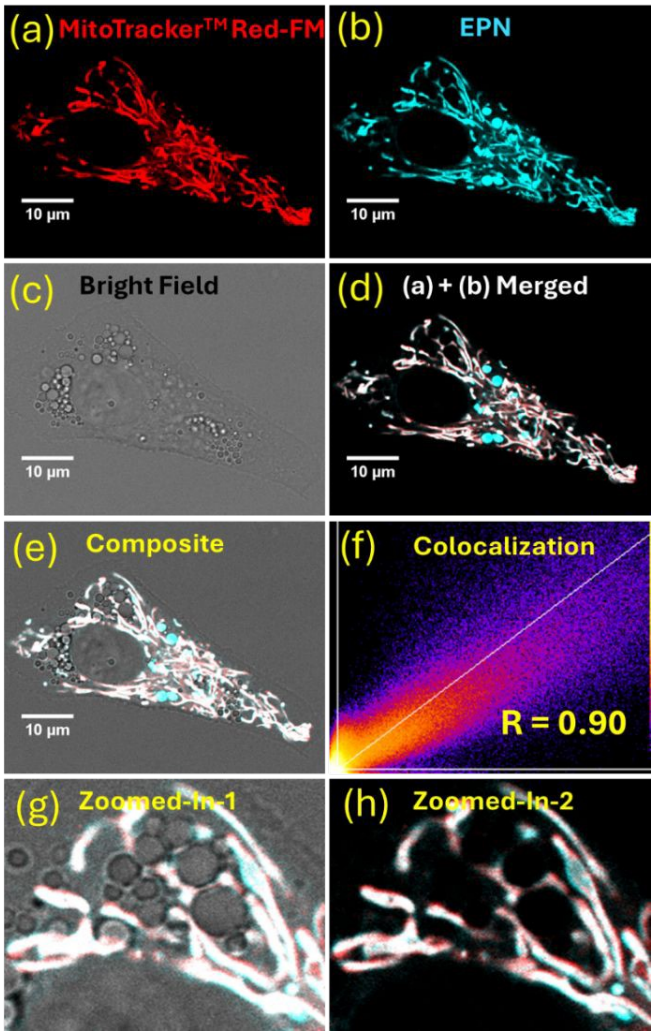

Figure 4. Fluorescence confocal microscopy images of HepG2 cells stained with MitoTracker™ Red FM (200 nM) and **EPN** (4 µM). Images from (a) to (h) represents MitoTracker™ Red FM (a), **EPN** (b), bright field (c), merged of two dyes (d), and composite image (e). Figure (f) shows the colocalization map and g-h represents zoomed-in images of the d and e, respectively. MitoTracker™ Red FM was excited at 570 nm and the emissions were collected from 580 nm to 700 nm. **EPN** was excited with 405 nm laser line and the emission was collected from 480 nm to 560 nm.

Conclusions

In summary, a highly biocompatible blue-green emitting pyridinium-based styryl dye (**EPN**) was synthesized in good yields for visualizing mitochondria in live cells. **EPN** exhibited a large Stokes' shift (Δλ >100 nm) due to strong ICT occur via π-acceptor system. The impact of the

ICT was studied extensively by low-temperature fluorescence which confirmed the contribution of ICT on the observed large Stokes' shift. **EPN** was readily excitable with a commercially available laser line (i.e., 405 nm) which produced bright-green visualization on stained HepG2 cells. The excellent mitochondria specificity of **EPN** was confirmed by fluorescence microscopy-based colocalization (calc. Pearson's colocalization constant =0.9) studies. **EPN** also exhibited the ability to produce stable fluorescence signal from stained cells for long time periods (I.e., up to 5 hours) confirming its suitability as a long-term imaging probe. **EPN** was exposed to continuous laser irradiation (405 nm) to assess its photostability and the probe exhibited over ~85 % fluorescence recovery after 30 minutes exhibiting an excellent photostability. Cell viability assessment also provided supporting evidence to confirm biocompatibility of **EPN** for live cell imaging experiments. When considering, structural simplicity, well resolved excitation/emission profiles, excellent photostability and biocompatibility, **EPN** will be a promising small-molecule imaging probe for biomedical imaging applications.

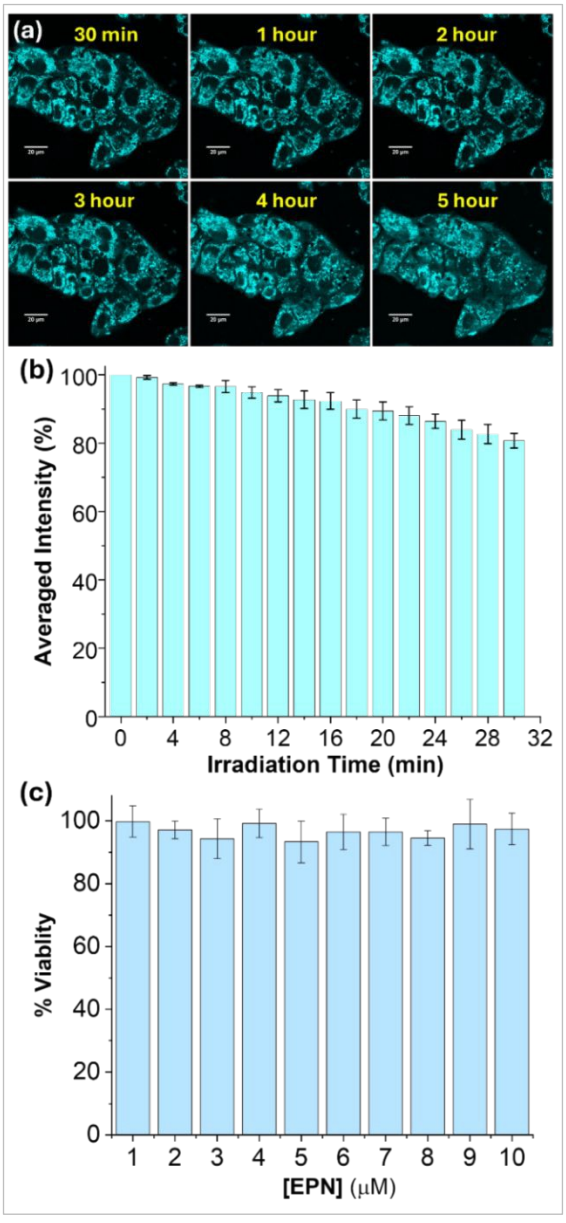

Figure 5. (a)-Fluorescence confocal microscopy images of HepG2 cells stained with **EPN** (4 μM). Images were obtained for 5 hours. Scale bar is 10 μm. Figure (b) represents the averaged fluorescence intensity (recovered) calculated after the continuous irradiation of **EPN** (4 μM) stained cells for 30 minutes. Figure (c) represents the cell viability data obtained for EPN by CellTiter-Glo® luminescent cell viability assay.

Conflicts of interest

There are no conflicts to declare.

Data availability

A The data supporting this article have been included as part of the Supplementary Information.

Author contributions

Conceptualization, C.S.A..; methodology, C.S.A., Y.P., R.V.S., K.J.W., and K.M.A.; validation, C.S.A., K.J.W., and K.M.A.; formal analysis, C.S.A.,K.M.A., and K.J.W.; investigation, C.S.A.,K.M.A., and K.J.W.; resources, C.S.A., Y.P., and R.V.S.; data curation, C.S.A., K.J.W., and K.M.A.; writing—original draft preparation, C.S.A, and K.J.W.; writing—review and editing, C.S.A., and K.J.W.; supervision, C.S.A., Y.P., R.V.S., and K.J.W.; project administration, C.S.A.; funding acquisition, C.S.A. All authors have read and agreed to the published version of the manuscript.

Notes and references

1 G. Y. Wiederschain, *Biochemistry (Moscow)*, 2011, **76**, 1276–1277.
2 J. Zhang, R. E. Campbell, A. Y. Ting and R. Y. Tsien, *Nat Rev Mol Cell Biol*, 2002, **3**, 906.
3 M. S. T. Gonçalves, *Chem Rev*, 2008, **109**, 190–212.
4 C. S. Abeywickrama, *Chemical Communications*, 2022, **58**, 9855–9869.
5 G. Jacquemet, A. F. Carisey, H. Hamidi, R. Henriques and C. Leterrier, *J Cell Sci*, 2020, **133**, jcs240713.
6 M. Fernández-Suárez and A. Y. Ting, *Nat Rev Mol Cell Biol*, 2008, **9**, 929.
7 M. V. Sednev, V. N. Belov and S. W. Hell, *Methods Appl Fluoresc*, 2015, **3**, 42004.
8 Z. Zhang, G. Zhang, J. Wang, S. Sun and Z. Zhang, *Comput Theor Chem*, 2016, **1095**, 44–53.
9 N. I. Wickramasinghe, B. Corbin, D. Y. Kanakarathna, Y. Pang, C. S. Abeywickrama and K. J. Wijesinghe, *Biosensors (Basel)*, 2023, **13**, 799.
10 L. Yuan, W. Lin and H. Chen, *Biomaterials*, 2013, **34**, 9566–9571.
11 X. Peng, F. Song, E. Lu, Y. Wang, W. Zhou, J. Fan and Y. Gao, *J Am Chem Soc*, 2005, **127**, 4170–4171.
12 W. Zhang, X. Zhao, W. Gu, T. Cheng, B. Wang, Y. Jiang and J. Shen, *New Journal of Chemistry*, 2018, **42**, 18109–18116.
13 C. S. Abeywickrama and Y. Pang, *Tetrahedron Lett*, 2016, **57**, 3518–3522.
14 V. S. Patil, V. S. Padalkar, K. R. Phatangare, V. D. Gupta, P. G. Umape and N. Sekar, *J Phys Chem A*, 2011, **116**, 536–545.

View Article Online
DOI: 10.1039/D4NJ05398B

Data availability

A The data supporting this article have been included as part of the Supplementary Information.